

Anti-cooperativity in hydrophobic interactions: A simulation study of spatial dependence of three-body effects and beyond

Seishi Shimizu and Hue Sun Chan^{a)}

Department of Biochemistry and Department of Medical Genetics and Microbiology, Faculty of Medicine, University of Toronto, Toronto, Ontario, M5S 1A8, Canada

(Received 9 March 2001; accepted 25 April 2001)

To better understand the energetics of hydrophobic core formation in protein folding under ambient conditions, the potential of mean force (PMF) for different three-methane configurations in an aqueous environment is computed by constant-pressure Monte Carlo sampling using the TIP4P model of water at 25 °C under atmospheric pressure. Whether the hydrophobic interaction is additive, cooperative or *anti-cooperative* is determined by whether the directly simulated three-methane PMF is equal to, more favorable, or less favorable than the sum of two-methane PMFs. To ensure that comparisons between PMFs are physically meaningful, a test-particle insertion technique is employed to provide unequivocal correspondence between zero PMF value and the nonexistent inter-methane interaction (zero reference-state free energy) experienced by a pair of methanes infinitely far apart. Substantial deviations from pairwise additivity are observed. Significantly, a majority of the three-methane configurations investigated exhibit anti-cooperativity. Previously simulated three-methane PMFs were defined along only one single coordinate. In contrast, our technique enables efficient computation of a three-methane PMF that depends on two independent position variables. The new results show that the magnitude and sign of nonadditivity exhibit a prominent angular dependence, highlighting the complexity of multiple-body hydrophobic interactions. Packing consideration of crystal-like constructs of an infinite number of methanes and analysis of methane sublimation and hydration data suggest that anti-cooperativity may be a prevalent feature in hydrophobic interactions. Ramifications for protein folding are discussed.

© 2001 American Institute of Physics. [DOI: 10.1063/1.1379765]

I. INTRODUCTION

The hydrophobic effect is one of the major driving forces in protein folding.^{1–3} Typically, many nonpolar amino acid side chains cluster together to form the hydrophobic cores of native proteins. To understand the physical principle of hydrophobic core formation as well as the role of nonpolar interactions in maintaining relatively compact protein denatured states,^{4–8} it is natural and necessary to decipher the energetics of multiple-body hydrophobic interactions.⁹ Here we take an incremental step toward this goal by first focusing on a model system of three methane molecules in water.

The principal complexity of multiple-body hydrophobic interactions is that they may not be amenable to a description in terms of simple pairwise sums of two-body free energies.^{10,11} The qualitative distinction between many-body and two-body associations of nonpolar chemical groups has long been known, and has sometimes been referred to as “bulk” versus “pair” hydrophobic interactions.⁹ In the present work, we define additivity, cooperativity or anti-cooperativity of multiple-body hydrophobic interactions by whether the total free energy of association among a set of N solutes ($N > 2$) is equal to, more favorable, or less favorable

than the sum of free energies of association of all $N(N - 1)/2$ possible pairings of the solutes computed one pair at a time at the two solutes' given positions while ignoring the effects of all $N - 2$ other solutes.

Elucidation of many-body hydrophobic interactions is of central importance to gaining insight into many remarkable properties of proteins. For instance, it has recently been shown that within the framework of self-contained heteropolymer chain models, additive hydrophobic effects alone are not sufficient to account for the experimentally observed calorimetric two-state behavior of many small proteins.^{12,13} This raises the question as to what degree current “big-picture” conceptions of balance of forces in proteins are adequate for rationalizing generic protein properties,¹⁴ necessitating research into the role of cooperative interactions in protein thermodynamics^{12,15} and folding kinetics.¹⁶

A number of researchers have investigated whether multiple-body hydrophobic interactions are additive. From a comparison between second and third virial coefficients, Kozak *et al.*¹⁷ reported that three-body hydrophobic interactions are anti-cooperative. In other words, they are weaker (less favorable to association) than the sum of their pairwise hydrophobic interaction components. However, a virial coefficient^{9,17} is a spatial integral of a function of the potential of mean force (PMF, or effective interaction free energy) over solute configurations. PMF can take both favorable (negative) and unfavorable (positive) values depending on

^{a)}Corresponding author. Department of Biochemistry, Faculty of Medicine, University of Toronto, Medical Sciences Building, 5th Floor, 1 King's College Circle, Toronto, Ontario, M5S 1A8, Canada. Telephone: 416-978-2697. Fax: 416-978-8548.

Electronic-mail: chan@arhenius.med.toronto.edu

the configuration of the hydrophobic solutes. Therefore, virial coefficients alone cannot tell us whether the effective interaction among a set of hydrophobic solutes in a specific configuration is additive or not.¹⁸ Currently, this information can only be inferred from model simulations.

Computer simulations of nonpolar solutes in water show that aggregation occurs only when solute concentration is sufficiently high.^{19–22} But it is not straightforward to ascertain from these simulations whether hydrophobic interactions themselves are pairwise additive. This is because hydrophobic aggregation in these model solutions, in which solutes are free to take up any configuration, is driven not only by the favorable effective interactions among the solutes but also by the lowered entropic cost of demixing at higher solute concentrations. In their insightful and systematic study of concentration dependent aggregation, the term “cooperativity” has been used by Tsai *et al.*²² to describe hydrophobic association. For the sake of clarity, it is important to emphasize here that the Tsai *et al.* “cooperativity” is *not* defined by a comparison between actual and hypothetical effective interaction strengths among the same number of hydrophobic solutes. Rather it refers to the more favorable total effective interactions among a larger cluster than that among a smaller cluster of hydrophobic solutes, a feature necessary for solute aggregation. As such, the meaning of the Tsai *et al.* “cooperativity”²² is different from the present definition. In principle, aggregation at high solute concentrations can occur not only with cooperative (present meaning) and additive effective interactions but also with mildly anti-cooperative effective interactions among the solutes.²³ Therefore, the observation of aggregation *per se* does not tell us whether the interactions among solutes are cooperative (present meaning) or not. The usage of the term cooperativity in the present article is identical to that of Czaplewski *et al.*²⁴

Two recent studies directly addressed the issue of cooperativity in multiple-body hydrophobic interactions. Unfortunately, their results disagree. Using free energy perturbation (FEP), Rank and Baker²⁵ compared three-methane and multiple-methane PMFs with two-methane PMF and found that when the methanes are in contact, the effective interactions are anti-cooperative (see their Figs. 4 and 6). On the other hand, a subsequent investigation by Czaplewski *et al.*²⁴ using the weighted histogram analysis method (WHAM) concluded that there are small cooperative effects for the three-methane effective interaction at the contact PMF minimum (see their Figs. 7 and 8). Adding to this puzzling contradiction are attempts to rationalize these results using different theoretical approaches. On one hand, Hummer²⁶ developed a modified PMF expansion of hydration free energy that successfully reproduced the *anti-cooperative* 14-methane PMF of Rank and Baker.²⁵ On the other hand, Czaplewski *et al.*²⁴ stated that their *cooperative* three-body PMF is consistent with molecular surface area considerations.

As far as simulation techniques are concerned, WHAM is often considered to be a method superior to FEP because errors do not accumulate with increasing solute–solute separation.²⁷ Both of these seminal studies, however, were based on somewhat arbitrary assumptions that PMFs or dif-

ferences between PMF values converge to zero at a certain finite separation between methanes. Specifically, Rank and Baker²⁵ assumed that all PMFs converge to zero when methane–methane separation is at 12.0 Å. Czaplewski *et al.*²⁴ assumed that their cooperativity term, i.e., the difference between three-methane PMF and its hypothetical additivity-based counterpart, becomes zero at around 7.5 Å to 8.5 Å. Assumptions such as these regarding what constitutes a zero-PMF baseline are not well justified, but they are probably unavoidable in the context of the methodologies used. We have recently overcome this problem by adopting a test-particle insertion technique, and have demonstrated that inaccurate treatments of zero-PMF baselines can lead to large errors.^{28,29} In the course of our investigation, we have also highlighted the fact that in order to meaningfully *compare* different PMFs (e.g., in calculating entropy and heat capacity from free energy as well as the additivity consideration here), an accurate determination of zero-PMF baselines is imperative.^{28,30} Here we apply the test-particle insertion technique to the computation of three-methane PMFs.

Three-methane PMFs have previously been simulated for two classes of methane configurations: (1) a single methane approaching a fixed methane dimer along a direction perpendicular to the axis connecting the centers of the two-methanes making up the dimer,^{24,25} and (2) three methanes at the vertices of an equilateral triangle approaching one another symmetrically.²⁴ Methane configurations in either class (1) or (2) are controlled by only one coordinate. Thus the configurational variation studied so far is quite limited. The test-particle insertion protocol employed in the present work not only provides an unequivocal determination of zero-PMF baselines, it also allows for a broader coverage of the three-methane free energy landscape. Here we study an extension of class (1), allowing one methane to take up positions other than that on the plane perpendicular to the methane dimer axis. This gives rise to a three-methane PMF that depends on two position variables, for one of the methanes may situate at any direction relative to the dimer axis. The corresponding angular variation of nonadditivity is reported below.

II. COMPUTATIONAL METHODS

A. Calculation of potentials of mean force by test-particle insertion

All results in this work are obtained by constant-pressure, constant-temperature (*NPT*) Monte Carlo simulations of 396 TIP4P water molecules at 25 °C (298.15 K) under atmospheric pressure in a box with periodic boundary conditions using BOSS version 4.1.³¹ We use a united-atom representation for the methanes. The simulation methodology as well as all numerical parameters used in this paper are the same as that in Shimizu and Chan.²⁸ A background review of PMF can also be found in the same reference.²⁸

Our model system is shown in Fig. 1. The configurations considered in the methane trimer studies of Rank and Baker²⁵ and the three-methane $2m+m$ investigation of Czaplewski *et al.*²⁴ correspond to the special case when $\phi = 0$. To establish a connection with and help resolve the contradiction between these prior studies, we first treat the ϕ

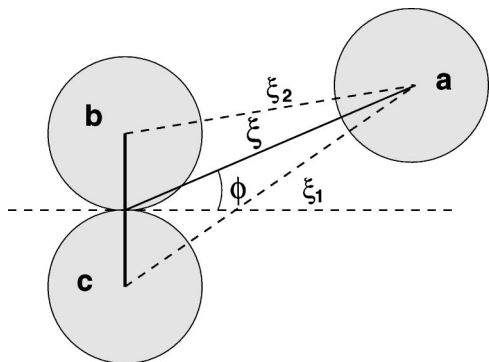


FIG. 1. Variables used in the present investigation to define the position of one methane (a) relative to the fixed methane dimer (b), (c). Methanes are represented by shaded spheres; water molecules are not depicted. Energetic and geometric parameters of the model methane and water molecules are identical to that of Shimizu and Chan (Ref. 28).

=0 situation. Subsequently we extend our discussion to a number of $\phi \neq 0$ cases that have not been investigated before.

As in Shimizu and Chan,²⁸ we employ a test-particle insertion approach. Three-methane PMFs are obtained from two independently calculated (pseudo-)chemical potentials, viz.,

$$\text{PMF} = \Delta G(\xi, \phi) = \mu_{abc}^*(\xi, \phi) - \mu_a^*, \quad (1)$$

where $\mu_{abc}^*(\xi, \phi)$ is the free energy of insertion of methane *a* into the aqueous environment at a location ξ , ϕ relative to the fixed methane dimer *b, c* (as defined in Fig. 1) and μ_a^* is the reference-state free energy of inserting a single methane molecule into pure water. The single-methane μ_a^* is obtained independently and not affected by the three-methane calculation. Clearly, $\mu_a^* = \lim_{\xi \rightarrow \infty} \mu_{abc}^*(\xi, \phi)$ because placing a single methane in water at a position infinitely far away from a methane dimer should lead to the same free energy change as placing the single methane into pure water. Therefore, in the formulation given by Eq. (1), the PMF between a single methane and a methane dimer infinitely far apart is guaranteed to be zero, as it should. This procedure thus determines zero-PMF baselines accurately and unambiguously. The reference-state single-methane hydration free energy μ_a^* in pure water has been determined to be 2.34 ± 0.05 kcal/mol at 25 °C under atmospheric pressure for the present model.²⁸

The three-methane quantity $\mu_{abc}^*(\xi, \phi)$ is obtained by using the relation

$$\mu_{abc}^*(\xi, \phi) = -kT \ln \left[\frac{\langle V \exp\{-\beta[U_a + U_{abc}(\xi, \phi)]\} \rangle_{N, bc}}{\langle V \rangle_{N, bc}} \right], \quad (2)$$

where kT is Boltzmann's constant times absolute temperature, V is the total volume of the model system, and $\langle \dots \rangle_{N, bc}$ denotes averaging in the ensemble of $N=396$ water molecules with the methane dimer *b, c*. U_a is the interaction energy between methane *a* and all the water molecules, whereas $U_{abc}(\xi, \phi)$ is the direct interaction energy between methane *a* and the methane dimer *b, c* [cf. Eq. (35) in Shimizu and Chan²⁸]. To calculate Eq. (2) by Monte Carlo simulation, we first generate a large collection of configura-

tions of a methane dimer plus water molecules. In each run, at least 1.3×10^5 initial passes are discarded, then coordinates or snapshots of the methane dimer solution are collected every 10 passes over a course of 6.4×10^7 passes. (In the present simulations, 1 pass equals 396 Monte Carlo steps.) Insertions are then attempted at six ϕ values ($\phi = n\pi/12$, $n=0, 1, \dots, 5$). Here 1,000 insertions for each angular value ϕ are attempted per snapshot to estimate the ensemble averages in Eq. (2).

B. Nonadditivity of three-methane potentials of mean force

The sign and magnitude of the deviation from additivity are determined by comparing the simulated three-methane PMF [Eq. (1)] with the *hypothetical* potential of mean force,

$$\Delta G_{\text{add}}(\xi, \phi) = \Delta G_2(\xi_1) + \Delta G_2(\xi_2), \quad (3)$$

calculated by assuming pairwise additivity. Here $\Delta G_2(\xi_1)$ or $\Delta G_2(\xi_2)$ is the two-methane PMF for a pair of methanes at a distance ξ_1 or ξ_2 apart (see Fig. 1). We have determined ΔG_2 previously using test-particle insertion techniques (Fig. 2 in Shimizu and Chan²⁸). We define the cooperative term as the actually simulated three-methane PMF in Eq. (1) minus the pairwise-additivity-based hypothetical PMF, viz.,

$$\text{cooperative term} = \Delta G(\xi, \phi) - \Delta G_{\text{add}}(\xi, \phi). \quad (4)$$

If this term is zero for a particular ξ , ϕ , the three-methane interaction is additive at the given position. Otherwise the three-methane interaction is nonadditive, then it is either cooperative or anti-cooperative depending on whether the cooperative term in Eq. (4) is negative or positive. As stated above, the present definition of the cooperative term is equivalent to that of Scheraga and co-workers²⁴ [see their Eq. (15)].

III. RESULTS AND DISCUSSION

A. Anti-cooperativity for $\phi=0$

Figure 2 shows the $\phi=0$ three-methane PMF. For nearly all positions shown ($\xi < 13$ Å), we find that the three-body PMF lies higher than the additivity-based hypothetical PMF. In other words, three-body interactions along a $\phi=0$ path of approach are mostly anti-cooperative, meaning that the actual interactions among the methanes are less favorable to hydrophobic association than that predicted by pairwise additivity.

The depth of the three-methane contact minimum is approximately -1.2 kcal/mol, which is shallower than the value of ≈ -1.35 kcal/mol by assuming additivity. The desolvation barrier is at $\xi \approx 5.5$ Å, slightly larger than the additivity-predicted $\xi = 5.4$ Å. The height of the desolvation barrier ($\approx +0.56$ kcal/mol) is significantly higher than the additivity prediction of $\approx +0.42$ kcal/mol. The first solvent-separated minimum from our simulation ($\xi \approx 7$ Å) is very shallow at ≈ -0.05 kcal/mol, in sharp contrast with the much deeper value of -0.24 kcal/mol if additivity were applicable. To ensure accuracy of our simulations, Fig. 2 compares the PMF deduced from the complete set of simulation data we have obtained and the corresponding PMF deduced

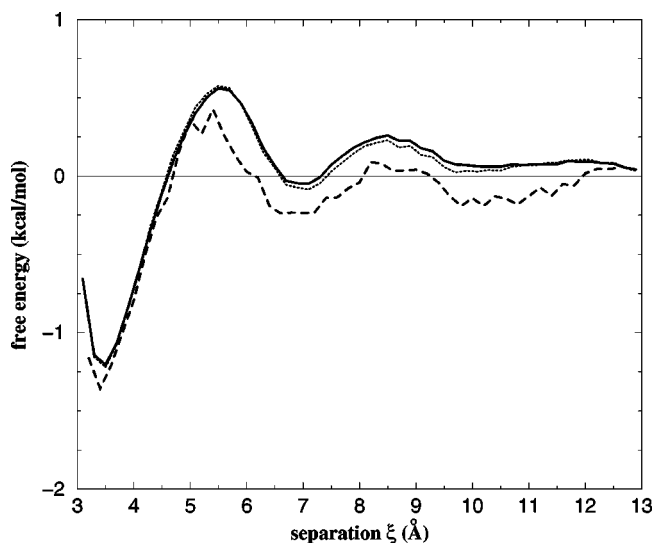


FIG. 2. Three-body PMF for bringing a single methane from infinity along a $\phi=0$ direction to a finite distance ξ away from the fixed methane dimer, computed using the test-particle insertion method described in the text [solid curve, Eq. (1) in Sec. II]. The hypothetical PMF [Eq. (3)] obtained by assuming additivity is given by the dashed curve. We assess the accuracy of this calculation by comparing the final full-simulation result (averaged over 6.4×10^7 passes; solid curve) with the half-simulation result (averaged over 3.2×10^7 passes; dotted curve). It is noteworthy that at positions where nonadditivity is substantial, the differences between the full- and half-simulation results are much smaller than the nonadditivity observed (differences between the solid and dashed curves). The present distance variable ξ is equivalent to the variable d in Rank and Baker (Ref. 25) whereas the m - m distance in Czaplewski *et al.* (Ref. 24) is equivalent to ξ_1 ($=\xi_2$ for $\phi=0$; see Fig. 1).

from half of the simulation data. The agreement is excellent, with deviations less than 0.005 kcal/mol. This lends support to the reliability of the nonadditivity effects observed in Fig. 2 as reproducible predictions of the model.

The present observation of anti-cooperativity at the contact minimum agrees qualitatively with the prediction by Rank and Baker²⁵ but disagrees with the prediction of cooperativity by Czaplewski *et al.*²⁴ Our three-methane contact minimum of ≈ -1.2 kcal/mol is close to that of Rank and Baker²⁵ (≈ -1.1 kcal/mol). In contrast, the contact minimum of Czaplewski *et al.*²⁴ is much deeper (≈ -1.5 kcal/mol). At larger methane separation ξ , the present simulation result differs from both previous studies. The height of the three-methane desolvation barrier obtained by Czaplewski *et al.*²⁴ is $\approx +0.2$ kcal/mol, which is significantly lower than our value of $\approx +0.56$ kcal/mol. Figure 2 shows substantial anti-cooperativity at the solvent-separated minimum (see above), but Rank and Baker²⁵ predicted a slight cooperativity for the same position. Their three-body PMF at the solvent-separated minimum is about -0.3 kcal/mol, which is significantly lower than our value of ≈ -0.05 kcal/mol in Fig. 2.

Figure 2 indicates significant anti-cooperativity of ~ 0.15 – 0.2 kcal/mol from $\xi \approx 5.5$ – 11.5 Å, covering the desolvation barrier and the first and second solvent-separated minima region of the hypothetical additivity-based PMF. This prediction differs significantly with both Rank and Baker²⁵ and Czaplewski *et al.*,²⁴ as both have reported near-

additivity for this region. Interestingly, the destabilization of the first solvent-separated minimum in Fig. 2 and the rather long spatial range of anti-cooperative effects associated with it are reminiscent of the results from a prior investigation of the effects of a nonpolar wall on a neon atom in water.³² Using a test-particle insertion method and the SPC water model, Forsman and Jönsson showed that the first solvent-separated minimum between two neon atoms is slightly stable (PMF <0), but the solvent-separated minimum between a neon and a nonpolar wall, as well as an extended region with larger neon–wall separations, have positive PMFs.³² At a most intuitive level of consideration, one may expect the interaction of a methane dimer with a single methane at a $\phi=0$ position sufficiently far away would be slightly more similar to the interaction between a nonpolar wall and a single methane in comparison with the interaction between a methane pair separated by the same distance. It seems reasonable, therefore, to suspect an intriguing connection between the effect observed by Forsman and Jönsson³² and the extended $\xi > 5.5$ Å anti-cooperativity region in Fig. 2 that includes part of the desolvation barrier and beyond.

A major source of uncertainty in the studies of Rank and Baker²⁵ and Czaplewski *et al.*²⁴ is the absence of a well-justified means to established zero-PMF baselines. This problem has been recognized by both groups, and Rank and Baker²⁵ have stated that their results are subjected to a possible zeroing error of 0.2–0.3 kcal/mol. The zero-PMF baseline uncertainty is essentially eliminated by the test-particle insertion technique employed here.²⁸ Our results also indicate that assumptions previously used for PMF zeroing are not generally valid. For example, Czaplewski *et al.*²⁴ posited that nonadditivity vanishes at relatively small separations of $\xi_1 = 7.5$ to 8.5 Å. (The corresponding ξ values are even smaller, because $\xi_1 > \xi$ for $\phi=0$; see Fig. 1.) However, this presumption is not supported by the present analysis. Figure 2 shows that substantial nonadditivity persists to much larger separations until $\xi \approx 12$ – 13 Å, thus casting doubt on the Czaplewski *et al.*²⁴ method of ascertaining cooperative effects.

In addition to the zero-PMF baseline issue, there are probably other reasons for the discrepancies among the simulation results as well, though other sources of disagreement are less apparent. One possibility is that there is a tendency for errors to accumulate in the FEP method used by Rank and Baker,²⁵ especially at relatively low simulation temperatures $\sim 25^\circ\text{C}$.²⁸ Rank and Baker²⁵ have reported convergence problems in the FEP computation of their 14-methane cluster, and larger random errors at larger methane–methane separations in their two- and three-body PMF calculations. Possible correlations in PMF errors at spatial positions close to one another may affect the accuracy of FEP (which relies on an integration pathway) and WHAM (which relies on overlap analyses). The present test-particle insertion technique should be more accurate not only because it offers justifiable zero-PMF baselines but also because it determines PMF values at different methane–methane separations independently.

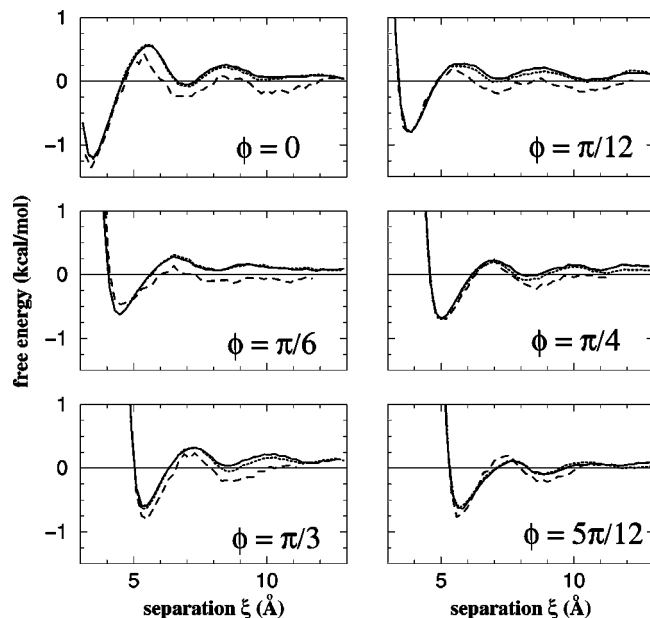


FIG. 3. Angular dependence of potential of mean force. PMFs (solid, dotted curves) are computed along six ϕ directions as indicated [Eq. (1)], and compared to hypothetical PMFs obtained by assuming additivity [dashed curve, Eq. (3)]. Line styles have the same meaning as that in Fig. 2. Among all cases considered, the differences between the full- and half-simulation PMF results are less than 0.08 kcal/mol, which are negligible for the most part in comparison to the nonadditivity effect observed.

B. Angular dependence of potential of mean force

We now extend our discussion to $\phi \neq 0$. Clearly, by symmetry, a ϕ (in radian) position is equivalent to positions at $-\phi$, $\pi - \phi$, and $\phi - \pi$. So only the range $0 \leq \phi \leq \pi/2$ needs to be considered to cover all possible methane configurations in Fig. 1.

Figure 3 shows PMFs for $\phi = n\pi/12$ ($n = 1, 2, 3, 4$ and 5, and the $n=0$ case in Fig. 2 is included for comparison). For each value of ϕ considered, PMF is calculated from test-particle insertions on the surface of a cone (which reduces to a plane for $n=0$). PMF for $\phi = \pi/2$ is not provided in the present work because it entails test-particle insertions along a line instead of on a surface. This reduces sampling and causes difficulties in achieving convergence of results for $\phi = \pi/2$.

Figure 3 shows that nonadditivity of three-methane PMF depends strongly on the direction of approach ϕ . In particular, the anti-cooperativity of the contact minimum decreases as ϕ is increased from 0 to $\pi/12$; and the interaction at the contact minimum becomes cooperative at $\pi/6$, changes to essentially additive at $\pi/4$, and then back to being anti-cooperative when ϕ is further increased to $\pi/3$ and $5\pi/12$. Remarkably, for all ϕ investigated, anti-cooperativity of various degree is observed at the solvent-separated minimum at $\xi = 7-9 \text{ \AA}$ (position depends on ϕ). This suggests that the extended region of anti-cooperativity observed for all angles considered in Fig. 3 may arise from similar physics (see above for the $\phi=0$ case), the microscopic origins of which, however, remain to be elucidated. The desolvation barrier is anti-cooperative as well for nearly all ϕ studied except that it is cooperative at $\phi = 5\pi/12$.

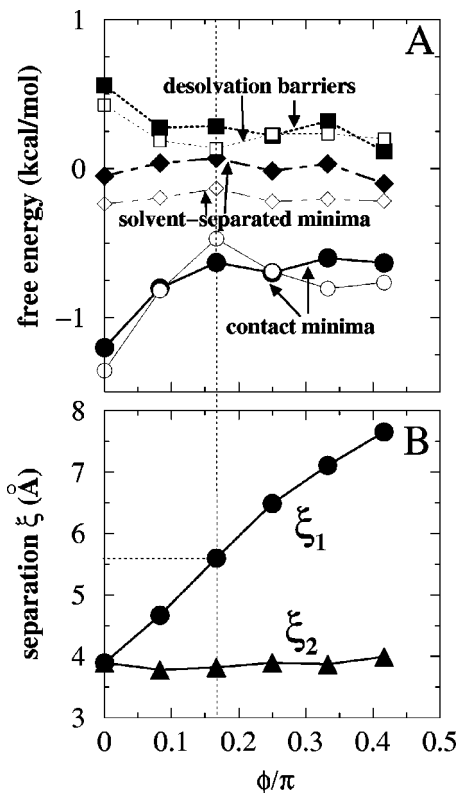


FIG. 4. Angular dependence of nonadditivity. (A) Three-methane PMF values vs ϕ (in units of π) from Fig. 3 at contact minima (circle, filled), desolvation barriers (square, filled), and solvent-separated minima (diamond, filled) [Eq. (1)] compared with their corresponding hypothetical additivity-based values (open symbols) [Eq. (3)]. (B) Distances between the single methane and each of the two methanes of the fixed methane dimer at three-methane contact minima as functions of ϕ (see Fig. 1 and the text for definitions). One of these distances, $\xi_2 \approx 3.8 \text{ \AA}$, is essentially independent of ϕ , whereas the other distance ξ_1 increases approximately linearly with ϕ . The vertical dotted line in (A) and (B) marks the angle $\phi = \pi/6$ at which the additivity-based hypothetical PMF [open circles in (A)] attains its peak value.

C. Angular dependence of nonadditivity

Figure 4(A) reports the angular trend of nonadditivity of three-methane PMF by focusing on the data in Fig. 3 for three representative classes of positions: (i) contact minima, (ii) desolvation barriers, and (iii) solvent-separated minima. These are, respectively, defined as the deepest minimum, the highest peak value, and the first minimum encountered when ξ is increased beyond the desolvation barrier in each of the PMF curves in Fig. 3.

Figure 4(A) shows that the height of the desolvation barrier is sensitive to ϕ . The barrier is highest at $\phi=0$ and significantly lower at other angles. Among the angles studied, we find that desolvation barrier is lowest along the most oblique angle of approach ($\phi = 5\pi/12$) that runs almost parallel to the axis of the methane dimer. This novel observation is suggestive of possible kinetic relevance. The role of hydrophobic desolvation barriers in protein folding kinetics remains to be better elucidated.^{25,28} Figure 4(A) also records an essentially ϕ -independent anti-cooperative effect of $\sim +0.25$ kcal/mol at all solvent-separated minima, as has been observed above for the $\phi=0$ case.

Angular dependence of nonadditivity at contact minima

TABLE I. Anti-cooperativity in the formation of extended close-packed regular structures of methanes from an aqueous environment.^a

	Close-packed methane structure I	Close-packed methane structure II	Experiment ^b
Nearest-neighbor			
methane–methane distance	3.8 Å	4.2 Å	4.2 Å
Interaction energy per methane ^c	−1.89	−2.46	−2.70 ^d
Hydration free energy ^e at 25 °C	+2.34	+2.34	+1.93
Free energy of formation of close-packed methane structure from water	−4.23	−4.80	−4.63
<i>Hypothetical</i> free energy of formation assuming pairwise additivity (theoretical) ^f	−7.20	−5.88	−5.88

^aEach of the two theoretical constructs (close-packed methane structures I and II) consists of an infinite number of methanes on a face-centered cubic lattice.

^bMethane crystal structure determined by x-ray investigation at temperatures $T \sim 17$ K is face-centered cubic with a nearest-neighbor methane–methane distance ≈ 4.2 Å (Ref. 33).

^cAll energies and free energies in this table are on a per methane basis and in units of kcal/mol.

^dSublimation data is from Syrkin and Dyatkina (Ref. 34) and Wannier (Ref. 35).

^eSimulated methane hydration free energy is from Shimizu and Chan (Ref. 28); experimental data is from Ben-Naim and Marcus (Ref. 36).

^fEach hypothetical free energy (bottom row) is a pairwise sum, of the test-particle simulated two-methane PMFs in TIP4P water (Ref. 28), over different methane–methane separations on the given face-centered cubic lattice. Note that each additivity-based hypothetical free energy, which depends on the nearest-neighbor methane–methane separation on the lattice, has a more negative value than the corresponding computed or experimental free energy listed above it, implying anti-cooperativity. See text for details.

is significant. This may help explain the finding of Pellegrini *et al.*¹⁰ that an approximation based on PMF additivity does not reproduce well the dihedral angle dependence of their simulated alanine dipeptide PMF. One feature of the ϕ -dependent contact-minima nonadditivity observed here may be rationalized by the following consideration. Figure 4(A) shows that PMF at contact minima is a smooth, almost monotonic function of ϕ . However, the additivity-based hypothetical PMF undergoes much sharper variations as a function of ϕ , and has a prominent maximum at $\phi \approx \pi/6$. This gives rise to the cooperativity of the three-methane contact–minimum interaction at $\phi = \pi/6$, a feature unique among the angles studied. The analysis in Fig. 4(B) shows that the hypothetical additive PMF peak at $\xi \approx \pi/6$ results from the fact that it is a sum of the favorable two-methane contact minimum PMF at $\xi_2 \approx 3.8$ Å on one hand and the highly unfavorable two-methane desolvation barrier PMF at $\xi_1 \approx 5.7$ Å (horizontal dotted line in B) on the other.²⁸ For the same reason the highest anti-cooperativity at desolvation barriers is recorded at $\phi = \pi/6$ as well. These examples illustrate how additivity can readily break down in multiple-body hydrophobic interactions.

On the whole, except for a small range of configurations where slight cooperativity or additivity is observed, our simulation predicts anti-cooperative interactions between a methane dimer and a single methane at most positions where they are in relatively close proximity ($\xi < 13$ Å).

D. A generalized case of anti-cooperativity in close-packed many-body hydrophobic interactions

To better understand the physical origin of the present results and to shed more light on the energetics of hydrophobic core formation in protein folding, we now take a first look beyond three-body hydrophobic interactions. In this en-

deavor, we find that much insight can be gained by considering the limiting case of an infinitely large crystal-like construct of methanes participating in infinitely-many-body interactions. As shown below, this approach is conceptually straightforward; the required computational effort is minimal and relevant experimental data is available (Refs. 33–36) to validate theoretical predictions.

Motivated by the fact that the two-methane PMF in water has a contact minimum when the methanes are 3.8 Å apart, we first consider a close-packed face-centered cubic lattice of methanes with nearest-neighbor distance of 3.8 Å (structure I in Table I). Clearly, no water can penetrate inside this lattice of methanes. So the interaction energy (cohesive energy) of any given methane with all other methanes in the lattice is readily calculated by using the model methane–methane Lennard-Jones potential alone and summing over all on-lattice pairwise distances. Therefore, the model interaction energy per methane of the lattice as a whole (Table I, entries on the second row) is equal to one half the cohesive energy of a methane. Model interaction energy per methane corresponds to experimentally measured heat of sublimation per methane extrapolated to $T \rightarrow 0$ K,³⁴ because the static theoretical lattice structures we are considering may be identified with a $T \rightarrow 0$ K crystal in which vibrational motions are minimized. It follows that the theoretically predicted free energy change per methane of forming this close-packed lattice structure by the thermodynamic process of bringing an infinite number of methanes at a set of initial positions infinitely far from each other (Table I, fourth row of entries) is equal to the lattice interaction energy per methane just calculated (Table I, second row of entries) minus the simulated hydration free energy of a single methane (Table I, third row of entries).

Now if the water-mediated interactions responsible for

the formation of the methane crystal from water were pairwise additive, the formation free energy per methane would be given by one half the sum of two-methane PMF values for all pairwise methane distances on the lattice. We have performed this calculation, which entails replacing the Lennard-Jones potential in the above calculation with the simulated two-methane PMF, the latter is available for a maximum methane-methane distance of 13 Å. The resulting hypothetical free energies are listed as the last row of entries in Table I. (We note that in the above calculation of lattice interaction energy using the Lennard-Jones potential alone, the error incurred by neglecting interactions between methanes that are more than 13 Å apart is negligible. Likewise, we expect the contribution to the hypothetical free energy from methane distances larger than 13 Å is negligible.)

A comparison between the free energy of formation of -4.23 kcal/mol and the hypothetical free energy of -7.20 kcal/mol based on assuming pairwise additivity (Table I) implies that the formation of a face-centered cubic lattice with a nearest-neighbor methane distance of 3.8 Å is highly anti-cooperative. This anti-cooperative effect amounts to $-4.23 + 7.20 = +2.97$ kcal/mol per methane. The main reason for this observation is rather simple. Without being surrounded by water, the model methane-methane interaction energy (in vacuum) has its minimum (most favorable) energy of ≈ -0.29 kcal/mol at a separation of ≈ 4.2 Å between the methanes. The pairwise interaction free energy minimum shifts to a separation of ≈ 3.8 Å when the methane-methane interaction is mediated by water; and the free energy minimum of ≈ -0.67 kcal/mol for the water-mediated interaction is significantly deeper than the corresponding interaction in the absence of water. Because the methane-methane Lennard-Jones potential becomes less favorable when methane-methane separation is smaller than ≈ 4.2 Å, a face-centered cubic methane crystal structure devoid of water with a nearest-neighbor distance of 3.8 Å is less stable than that with a nearest-neighbor distance of 4.2 Å (structure II in Table I, which also cannot accommodate water). But at a nearest-neighbor methane distance of 3.8 Å the hypothetical interaction based on the water-mediated PMF is very favorable. This gives rise to the large anti-cooperativity effect for this configuration. The conclusion from this general consideration is consistent with the finding of Rank and Baker²⁵ that the PMF of their face-centered cubic 14-methane cluster is significantly anti-cooperative around the contact minimum. The above analysis also rationalizes their result showing that the free energy minimum of their cluster occurs at a nearest-neighbor methane-methane distance (≈ 4.0 Å) larger than that (3.8 Å) of the two-methane PMF contact minimum, because water molecules are excluded from the interior of their cluster when the methanes are in close contact. In this perspective, the anti-cooperativity observed for the present three-methane $\phi = 0$ close-packed contact minimum (Fig. 2) may intuitively be viewed as the beginning of this general trend.

Since the two-methane PMF increases rapidly as methane-methane separation increases from 3.8 Å, anti-cooperativity is less prominent for the corresponding close-packed methane structure with a nearest-neighbor methane

distance equals 4.2 Å (structure II in Table I). Nevertheless, the formation of such a face-centered cubic methane structure from water is still significantly anti-cooperative ($-4.80 + 5.88 = +1.08$ kcal/mol per methane). Table I shows that the present model prediction of the free energy of formation (infinitely-many-body PMF) of a static crystal-like methane structure from 25 °C water (-4.80 kcal/mol per methane for structure II) agrees reasonably well with that deduced from experiments (-4.63 kcal/mol per methane). To further assess the physical reasonableness of these energies, it is instructive to compare them with nonatomistic empirical treatments of hydrophobic effects that employ solvent (water) accessible surface area (SASA).³⁷ If the SASA of a model methane is taken to be that of a sphere with a 3.3 Å radius²⁵ (136.8 Å²), the methane experimental data in Table I corresponds to an energetic favorability of 34 cal/mol/ per Å² of SASA buried, which is identical to that deduced from cyclohexane-water transfer data.³⁸ This agreement is reassuring, though SASA-based empirical approaches are known to be insufficient for describing nonadditivity effects and the spatial dependence of hydrophobic interactions^{24,25,28,30}

If one half of the nearest-neighbor distance between methanes is taken as the radius of each methane's van der Waals envelope,³⁹ the packing fraction of a face-centered cubic structure is equal to $\pi/\sqrt{18} = 0.7404\dots$, which is believed to be the densest possible for equal-sized spheres (Kepler's yet unproven conjecture). Typical organic crystals have packing fractions around this value. Results in Table I are pertinent to protein energetics because the packing fractions in protein cores are similar to those in organic crystals or even slightly higher.^{39,40} Therefore, our idealized packing analysis should provide indications as to whether the hydrophobic component of the interactions that drive protein core formation is cooperative. Because there is little uncertainty in the experimentally measured heat of sublimation and hydration free energy, the present conclusion regarding the prevalence of anti-cooperativity in hydrophobic interactions hinges on the accuracy of the simulated two-methane PMF. Obviously, further investigations should be conducted to ascertain the robustness of our general predictions, by testing their sensitivity to changes in modeling parameters, for example. Nonetheless, it should be pointed out that the magnitude of our contact minimum of ≈ -0.67 kcal/mol for the two-methane PMF at 25 °C²⁸ is not large among the published values in the literature, and a more favorable two-methane PMF would only lead to higher anti-cooperativity. For example, at ~ 25 °C (either at 298 K or 300 K), two-methane contact minimum has been reported to be approximately -1.04 kcal/mol,⁴¹ -0.75 kcal/mol,^{24,42} -0.7 kcal/mol,²⁵ and -0.50 kcal/mol.¹⁸ Furthermore, these other studies are less reliable because of their lack of certainty in zero-PMF baseline determination. These considerations have therefore led us to believe, at least at a qualitative level, that the anti-cooperativity phenomena reported here are a reasonably good reflection of reality.

IV. CONCLUSIONS

To summarize, we have determined the three-methane PMF between a single methane and a methane dimer by

applying a test-particle method that provides for an accurate and unambiguous zero-PMF baseline. The present results are more reliable and extensive than those from previous investigations. The three-methane PMF we obtained is a function of two coordinates, covering trends over nearly all possible configurations. We expect the broader view afforded by the new three-methane PMF to offer insight into the kinetics of hydrophobic association. A comparison of the present three-methane PMF with two-methane PMFs shows significant deviations from pairwise additivity. For most of the spatial arrangements of the methanes in our study, three-methane interactions are anti-cooperative. Their interactions are cooperative for only a narrow range of methane configurations. Experimental data on methane crystals and hydration and theoretical considerations all suggest strongly that anti-cooperativity is likely a general feature in the formation of tightly packed clusters from methane-size nonpolar solutes in an aqueous environment. This may imply that a major part of the thermodynamic two-state behavior of protein folding originates from interactions besides hydrophobic effects.^{12,13,15} A further effort is underway to relate the multiple-body hydrophobic interaction properties reported here with water structure and popular implicit solvent models.

ACKNOWLEDGMENTS

We thank Danny Heap for his effort in maintaining our computing system. This work was supported in part by the Connaught Fund, a Premier's Research Excellence Award from the Province of Ontario and Medical Research Council of Canada Grant No. MT-15323. One of the authors (H.S.C.) is a Canada Research Chair in Biochemistry.

¹W. Kauzmann, *Adv. Protein Chem.* **14**, 1 (1959).

²K. A. Dill, *Biochemistry* **29**, 7133 (1990).

³B. Honig and A.-S. Yang, *Adv. Protein Chem.* **46**, 27 (1995).

⁴T. R. Sosnick and J. Trehwella, *Biochemistry* **31**, 8329 (1992).

⁵D. Shortle, *Curr. Opin. Struct. Biol.* **3**, 66 (1993).

⁶Y. Hagihara, M. Hoshino, D. Hamada, M. Kataoka, and Y. Goto, *Folding Des.* **3**, 195 (1998).

⁷Y. K. Mok, C. M. Kay, L. E. Kay, and J. Forman-Kay, *J. Mol. Biol.* **289**, 619 (1999).

⁸M. Arai and K. Kuwajima, *Adv. Protein Chem.* **53**, 209 (2000).

⁹R. H. Wood and P. T. Thompson, *Proc. Natl. Acad. Sci. U.S.A.* **87**, 8921 (1990).

¹⁰M. Pellegrini, N. Gronbeck-Jensen, and S. Doniach, *J. Chem. Phys.* **104**, 8639 (1996).

¹¹V. Martorana, D. Bulone, P. L. San Biagio, M. B. Palma-Vittorelli, and M. U. Palma, *Biophys. J.* **73**, 31 (1997).

¹²H. S. Chan, *Proteins: Struct., Funct., Genet.* **40**, 543 (2000).

¹³H. Kaya and H. S. Chan, *Proteins: Struct., Funct., Genet.* **40**, 637 (2000).

¹⁴H. S. Chan, *Nature (London)* **392**, 761 (1998).

¹⁵H. Kaya and H. S. Chan, *Phys. Rev. Lett.* **85**, 4823 (2000).

¹⁶M. P. Eastwood and P. G. Wolynes, *J. Chem. Phys.* **114**, 4702 (2001).

¹⁷J. J. Kozak, W. S. Knight, and W. Kauzmann, *J. Chem. Phys.* **48**, 675 (1968).

¹⁸S. Lüdemann, R. Abseher, H. Schreiber, and O. Steinhauser, *J. Am. Chem. Soc.* **119**, 4206 (1997).

¹⁹D. C. Rapaport and H. A. Scheraga, *J. Phys. Chem.* **86**, 873 (1982).

²⁰A. Wallqvist, *J. Phys. Chem.* **95**, 8921 (1991).

²¹A. Wallqvist, *Chem. Phys. Lett.* **182**, 237 (1991).

²²J. Tsai, M. Gerstein, and M. Levitt, *Protein Sci.* **6**, 2606 (1997).

²³S. Shimizu and H. S. Chan, *J. Chem. Phys.* (in press).

²⁴C. Czaplewski, S. Rodziewicz-Motowidlo, A. Liwo, D. R. Ripoll, R. J. Wawak, and H. A. Scheraga, *Protein Sci.* **9**, 1235 (2000).

²⁵J. A. Rank and D. Baker, *Protein Sci.* **6**, 347 (1997).

²⁶G. Hummer, *J. Am. Chem. Soc.* **121**, 6299 (1999).

²⁷S. Kumar, D. Bouzida, R. H. Swendsen, P. A. Kollman, and J. M. Rosenberg, *J. Comput. Chem.* **13**, 1011 (1992).

²⁸S. Shimizu and H. S. Chan, *J. Chem. Phys.* **113**, 4683 (2000).

²⁹In contrast to PMF determination, the calculation of mean force [see, e.g., G. Ciccotti, M. Ferrario, J. T. Hynes, and R. Kapral, *Chem. Phys.* **129**, 241 (1989); and Refs. 10, 11, 28] is independent of shifts in the zero-PMF value. We focus here on the (scalar) nonadditivity of PMF, which requires accurate zero-PMF baselines, because it directly addresses issues of thermodynamic stability and cooperativity of multiple-body hydrophobic interactions (see Refs. 24, 25). In future investigations, however, it would be interesting to also explore vectorial nonadditivities of the hydration mean force.

³⁰S. Shimizu and H. S. Chan, *J. Am. Chem. Soc.* **123**, 2083 (2001).

³¹W. L. Jorgensen, BOSS, Version 4.1 Yale University, New Haven, CT, 1999.

³²J. Forsman and B. Jönsson, *J. Chem. Phys.* **101**, 5116 (1994).

³³A. Schallamach, *Proc. R. Soc. London, Ser. A* **171**, 569 (1939).

³⁴A. Syrkin and M. E. Dyatkina, *Structure of Molecules and the Chemical Bond* (Butterworths, London, 1950), p. 309.

³⁵G. H. Wannier, *Elements of Solid State Theory* (Cambridge University Press, Cambridge, 1959), p. 227.

³⁶A. Ben-Naim and Y. Marcus, *J. Chem. Phys.* **81**, 2016 (1984).

³⁷B. Lee and F. M. Richards, *J. Mol. Biol.* **55**, 379 (1971).

³⁸H. S. Chan and K. A. Dill, *Annu. Rev. Biophys. Biomol. Struct.* **26**, 425 (1997).

³⁹F. M. Richards, *J. Mol. Biol.* **82**, 1 (1974).

⁴⁰M. Levitt, M. Gerstein, E. Huang, S. Subbiah, and J. Tsai, *Annu. Rev. Biochem.* **66**, 549 (1997).

⁴¹S. W. Rick and B. J. Berne, *J. Phys. Chem. B* **101**, 10488 (1997).

⁴²M. Ikeguchi, S. Nakamura, and K. Shimizu, *J. Am. Chem. Soc.* **123**, 677 (2001).